

1 **Templated trimerization of the phage L decoration protein on capsids**

2

3 Running Title: Folding of phage L Dec protein

4

5 Brianna M. Woodbury¹, Rebecca L. Newcomer¹, Andrei T. Alexandrescu^{1*}, and Carolyn M.
6 Teschke^{1,2*}

7

8 *¹Department of Molecular and Cell Biology, University of Connecticut, 91 N. Eagleville Rd, Storrs,*
9 *CT, 06269-3125, USA*

10 *²Department of Chemistry, University of Connecticut, 55 N. Eagleville Rd, Storrs, CT, 06269-*
11 *3060, USA*

12

13 *CORRESPONDING AUTHORS:

14 Carolyn M. Teschke

15 E-mail: carolyn.teschke@uconn.edu

16 Andrei T. Alexandrescu

17 E-mail: andrei.alexandrescu@uconn.edu

18

19

20 **ABSTRACT**

21 The 134-residue phage L decoration protein (Dec) forms a capsid-stabilizing homotrimer that has
22 an asymmetric tripod-like structure when bound to phage L capsids. The N-termini of the trimer
23 subunits consist of spatially separated globular OB-fold domains that interact with the virions of
24 phage L or the related phage P22. The C-termini of the trimer form a three-stranded intertwined
25 spike structure that accounts for nearly all the interactions that stabilize the trimer. A Dec mutant
26 with the spike residues 99-134 deleted (Dec_{C1-98}) was used to demonstrate that the stable globular
27 OB-fold domain folds independently of the C-terminal residues. However, Dec_{C1-98} was unable to
28 bind phage P22 virions, indicating the C-terminal spike is essential for stable capsid interaction.
29 The full-length Dec trimer is disassembled into monomers by acidification to pH <2. These
30 monomers retain the folded globular OB-fold domain structure, but the spike is unfolded.
31 Increasing the pH of the Dec monomer solution to pH 6 allowed for slow trimer formation *in vitro*
32 over the course of days. The infectious cycle of phage L is only around an hour, however, implying
33 Dec trimer assembly *in vivo* is templated by the phage capsid. The Thermodynamic Hypothesis
34 holds that protein folding is determined by the amino acid sequence. Dec serves as an unusual
35 example of an oligomeric folding step that is kinetically accelerated by a viral capsid template.
36 The capsid templating mechanism could satisfy the flexibility needed for Dec to adapt to the
37 unusual quasi-symmetric binding site on the mature phage L capsid.

38

39

40

41

42

43

44

45

46

47 **KEYWORDS**

48 Bacteriophage, metastable state, misfolding, folding reversibility, virus

49

50 **ABBREVIATIONS**

51 cryoEM, cryogenic electron microscopy; WT, wild type; Dec, phage L decoration protein; Dec_{closed},
52 trimeric form with the three OB-fold domains interacting; Dec_{open}, trimeric form with the three OB-
53 fold domains not interacting; NDec, Dec construct with an N-terminal His₆ tag; Dec monomers,
54 Dec trimers incubated at pH <2 and returned to pH 6; OB-fold, oligonucleotide/oligosaccharide-
55 binding fold; NMR, nuclear magnetic resonance; HSQC, heteronuclear single-quantum
56 coherence; SDS, sodium dodecyl sulfate; TCA, trichloroacetic acid.

57

58 1. INTRODUCTION

59 Decoration proteins, also known as cementing proteins, non-covalently bind and stabilize
60 the capsids of some viruses and phages, as well as serving additional functions like participating
61 in target-cell recognition (Dedeo, Teschke, and Alexandrescu 2020). ‘Dec’ is a decoration protein
62 encoded by phage L (Dedeo, Teschke, and Alexandrescu 2020; Gilcrease et al. 2005; Newcomer
63 et al. 2019) that fortifies phage L virions *in vivo* against the large internal pressure resulting from
64 genome packaging (Gilcrease et al. 2005). Phage L Dec protein can also bind to phage P22
65 virions, as L and P22 coat proteins and capsid structures are nearly identical (Newcomer et al.
66 2019; Parent et al. 2012; Tang et al. 2006). Dec has an unusual phage binding mechanism,
67 preferring to bind as a homotrimer to specific capsid icosahedral quasi-three-fold sites that have
68 imperfect symmetry (Gilcrease et al. 2005; Newcomer et al. 2019). Thus, the three identical
69 protomers in the trimer must adopt slightly different conformations to optimize interactions with
70 the capsid.

71 [Figure 1A](#) shows A schematic of an icosahedral capsid with the preferred quasi-three-fold
72 sites for Dec binding that occur between hexons on the phage L capsids denoted as orange three-
73 petal flowers. The Dec trimer has a tripod-like structure ([Figure 1B](#)) with the three globular OB-
74 fold domains forming the legs that are the primary point of contact with the capsid ([Figure 1C](#)).
75 The structure of the monomeric OB-fold motif was solved by solution NMR and fits well to the 4.2
76 Å resolution electron density map of the trimer base in the cryoEM structure (Newcomer et al.
77 2019). Above the tripod base, there is a C-terminal spike formed by the last ~40 residues of each
78 subunit with a poorer (> 6Å) resolution in the cryoEM density due to its higher mobility. The C-
79 terminus is completely unfolded in Dec monomers indicating it only becomes structured when
80 Dec trimerizes (Newcomer et al. 2018; Newcomer et al. 2019) ([Figure 1B](#)). Since the resolution
81 of the spike was too low to allow cryoEM structure determination, its structure in the cryoEM data
82 was modeled as a three-stranded β -helix structure based on its cylindrical shape and remote
83 sequence homology to phage tail fiber proteins (Newcomer et al. 2019). Though the OB-fold

84 domains of Dec are individually very stable, there are few if any contacts between the OB-fold
85 domains in the capsid-bound trimer, suggesting its trimeric oligomerization state is stabilized
86 entirely by the C-terminal spike.

87 The vast majority of proteins have their native functional structure determined by their
88 amino acid sequence according to the Thermodynamic Hypothesis (Anfinsen 1973). In rare
89 cases, proteins can exist in multiple conformational states (Bryan and Orban 2010; Kaplan, Olson,
90 and Alexandrescu 2021; Porter, Artsimovitch, and Ramirez-Sarmiento 2024), with the
91 predominant species kinetically trapped in a metastable state corresponding to a sub-global
92 energy well (Ghosh and Ranjan 2020; Baker and Agard 1994). Metastable states often occur
93 when proteins shift between different environments (for example, a shift in pH), or undergo
94 structural changes coupled to binding. Examples of proteins that fold into metastable states
95 include serpin serine protease inhibitors, viral membrane fusogens such as hemagglutinin A, a
96 number of intrinsically disordered proteins that fold only in the presence of a binding partner, and
97 amyloidogenic proteins that often aggregate through metastable conformations (Ghosh and
98 Ranjan 2020).

99 Here we investigate the folding properties of the phage L Dec trimer. Information on the
100 folding of Dec is important both to understanding the biological functions of the protein (Gilcrease
101 et al. 2005; Newcomer et al. 2019; Tang et al. 2006), and since the Dec trimer has become a
102 popular carrier vehicle in nanotechnology applications such as molecular display on phage
103 surfaces and the design of novel nanomaterials (Dedeo, Teschke, and Alexandrescu 2020;
104 Parent et al. 2012; Schwarz et al. 2015; Goodall et al. 2021; Uchida et al. 2015). We show that
105 Dec freshly purified from an *Escherichia coli* heterologous expression system is trimeric and that
106 these trimers have a “closed” conformation (Dec_{closed}) inconsistent with the cryoEM structure of
107 the capsid-bound trimer (Newcomer et al. 2019) (Figure 1B). Dec_{closed} trimers can be
108 disassembled into monomers upon acidification. These Dec monomers retain a folded OB-fold
109 domain comprised of residues 12-89 but have unfolded N- and C-termini corresponding to

110 residues 1-11 and 90-134, respectively (Newcomer et al. 2019). In temperature melt experiments,
111 Dec monomers and the Dec₁₋₉₈ C-terminal truncation mutant (Figure 1D) were completely
112 unfolded at 63 °C in 5 M urea, with the unfolding of the OB-fold globular domain being reversible.
113 By contrast, reassembly of Dec monomers into trimers *in vitro* required days and the trimers are
114 consistent with a Dec_{open} state, where the OB-fold domains have rotational freedom rather than
115 the initial Dec_{closed} state. We propose that *in vivo* Dec trimerization is templated by the structure
116 of the capsid surface.

117

118 2. RESULTS

119 2.1 The Dec protein C-terminal tail is essential for binding to virions.

120 In the model of trimeric Dec used for cryoEM reconstruction of the complex between Dec
121 and phage L capsids (Newcomer et al. 2019), only the C-terminal tail forms contacts between the
122 protomers in the trimer (Figure 1C). This predicts that in the absence of phage in solution, the
123 globular OB-fold domains should have unrestricted rotational diffusion relative to each other
124 (Figure 1B). The unusual oligomeric structure of Dec led us to ask how the protein assembles
125 and the role of trimerization in binding to phage capsids.

126 To investigate if trimerization is essential for binding to phage capsids, a Dec truncation
127 mutant was used to remove the C-terminal tail by insertion of a stop codon at codon 99 in the *dec*
128 gene carried in an expression plasmid (Δ residues 99-134). (Figure 1D). The construct includes
129 an N-terminal hexa-histidine tag, denoted as “NDec” for the full-length protein or “NDec₁₋₉₈” for the
130 truncation mutant. Note, the N-terminal His₆-tag does not interfere with binding to capsids or
131 trimerization (Parent et al. 2012).

132 We first characterized the proteins in the absence of capsids by running them on a pH 8.5
133 native polyacrylamide gel (Figure 2A). Freshly purified Dec (no tag) migrated on the native gel at
134 a position consistent with being trimeric. Dec monomers (no tag) formed by incubation of Dec
135 trimers at pH 1 followed by return to pH 6 (hereafter referred to as “Dec monomers”) (Newcomer

136 et al. 2018) ran faster than the Dec trimers, as expected. NDec₁₋₉₈ ran faster than Dec monomers,
137 at a position consistent with it being monomeric, indicating that the C-terminal tail is necessary
138 for trimerization. [Figure 2B](#) shows ¹H-¹⁵N HSQC NMR spectra of NDec monomers (black)
139 (Newcomer et al. 2019; Newcomer et al. 2018) superimposed with the spectrum of NDec₁₋₉₈ (red).
140 In an HSQC spectrum, each crosspeak is due to the amide N-H pair from a specific amino acyl
141 residue in the protein. The close matches of chemical shifts in the superposed spectra indicate
142 that the structure of the OB-fold is nearly identical in the monomers where the C-terminus is
143 disordered and in NDec₁₋₉₈ where the C-terminus is deleted. The extra peaks in the Dec
144 monomers compared to NDec₁₋₉₈ are assigned to the C-terminal tail (Newcomer et al. 2019;
145 Newcomer et al. 2018) and have ¹H_N chemical shifts between 7.8 and 8.5 ppm characteristic of
146 unfolded structure. Thus, the C-terminal tail is not necessary for the folding of the N-terminal OB-
147 fold domain.

148 To investigate if the Dec protein needs to be trimeric to bind phage virions, trimeric NDec,
149 freshly prepared Dec monomers, and NDec₁₋₉₈ were each incubated with P22 phages for 15 min,
150 after which the samples were applied to CsCl step gradients to separate free Dec from P22-bound
151 Dec. The phage band was pulled from the gradient, the proteins were TCA precipitated, then
152 assessed by SDS-PAGE for the presence of Dec ([Figure 2C](#)). As previously reported, the trimeric
153 NDec bound to P22 virions (Parent et al. 2012), as did Dec monomers where the C-terminal tail
154 is unfolded. However, monomeric NDec₁₋₉₈ did not bind to P22 virions, indicating that the presence
155 of the C-terminal tail is essential for persistent binding ([Figure 2C](#)).

156

157 2.2 Unfolding and refolding of Dec trimers.

158 As described above, the C-terminal tail is needed for binding of monomer Dec to phages
159 heads, but do the Dec monomers undergo trimerization prior to capsid binding? To elucidate the
160 mechanism of Dec-capsid binding, experiments were first performed to better understand the
161 process of Dec folding, unfolding, and trimerization. To determine the long-term stability of WT

162 Dec_{closed} trimers near neutral pH, given that the trimers readily dissociate at acidic pH, the protein
163 was incubated at pH 6 and a temperature of 33 °C. Aliquots were taken at specific times and
164 analyzed by native PAGE. While Dec remained largely trimeric throughout the 96-hour time
165 course, some proteolysis did occur based on the appearance of low molecular weight bands after
166 48 hours (Figure 3A). This result suggests that the equilibrium favors trimers at pH 6. Dropping
167 the pH to 1 for 30 min caused trimeric Dec to dissociate into monomers (Figure 3B), indicating
168 that the equilibrium between trimers and monomers shifts towards monomers with decreasing
169 pH. The Dec trimers reassemble at pH 6, but over a very slow 96 h time period (Figure 3B).

170 We also examined the unfolding and refolding of WT Dec using NMR ¹H-¹⁵N HSQC
171 experiments to obtain information at the residue level. At the start of the experiment, freshly
172 purified trimeric WT Dec protein in pH 6 buffer at 33 °C showed only a few crosspeaks from the
173 N- and C-termini (Figure 4A, top left panel). The large size of the Dec trimer (43 kDa), as well as
174 possible additional conformational exchange contributions from a dynamic oligomerization
175 interface, broadened most of the NMR signals in the protein. After the initial HSQC spectrum was
176 obtained, the pH was lowered incrementally to pH 2 (indicated by the down arrow in Figure 4A),
177 and an HSQC spectrum was collected at each increment. Obtaining each spectrum took around
178 75 min. Additional crosspeaks were observed as the pH was decreased, ultimately resulting in
179 the conversion of Dec trimers into monomers at acidic pH. Of note, at pH 2 the HSQC spectrum
180 is consistent with the protein retaining a folded OB-fold domain structure but having unfolded N-
181 and C-termini (compare to Figure 2B). After incubation at pH 2, the pH was raised incrementally
182 (indicated by the up arrow in Figure 4), and an HSQC spectrum was collected. With increasing
183 pH, the spectra retained dispersed crosspeaks that were consistent with folded structure in the
184 OB-fold domains but a spectrum similar to the initial sample with broadened NMR signals was
185 not recovered.

186 Spectra were subsequently obtained at 3 hours and 96 hours after return to pH 6 (Figure
187 5A, B). Even after 96 hours, the crosspeaks remained dispersed and did not return to the initial

188 trimeric Dec_{closed} state shown in [Figure 4 \(top left\)](#) where only a few NMR signals were observed.
189 However, from the native gels shown in [Figure 3B](#), the protein had re-trimerized by this time. The
190 crosspeak intensities in the NMR spectrum undergo an ~50% drop in intensity that could be due
191 to an increase in size due to the reassociation of the monomers into trimers observed by native
192 gels over the 96-hour time period. The chemical shifts from the C-terminus remain invariant over
193 this time but there is a larger loss in NMR peak intensity than for the OB-fold segment ([Figure](#)
194 [5C](#)). This could be due to intermediate exchange broadening linked to a dynamic equilibrium
195 between dissociated and associated forms of the C-terminal spike, and/or anisotropic tumbling of
196 the rod-like structure. Thus, we conclude that the spectrum in [Figure 5B](#) is of Dec trimers, but in
197 a Dec_{open} state where the OB-fold domains have sufficient segmental rotational freedom to give
198 NMR spectra comparable to that of the 12.9 kDa NDec₁₋₉₈ fragment.

199 Our data indicate that the OB-fold domain is stable even in acidic conditions of pH 1-2.
200 Because of its high stability the OB-fold domain required incubation in 5 M urea and 63 °C to
201 achieve thermal unfolding ([Figure 6](#)). In [Figure 6A](#), Dec monomers were incubated in 5 M urea at
202 33 °C or 63 °C and compared by circular dichroism to Dec held at 33 °C without urea. Only the
203 data from 220 to 260 nm are shown as urea absorbs strongly further into the far UV. The positive
204 peak at 230 nm is unusual but is consistent with the presence of aromatic residues or disulfide
205 bonds (Andersson, Carlsson, and Freskgard 2001; Haas, MacColl, and Banas 1998). As there
206 are no cysteine residues in Dec, we attribute the peak to aromatic amino acids. In addition, there
207 is only a single aromatic residue (F120) in the C-terminal tail, and Dec₁₋₉₈ also shows the positive
208 peak at 230 nm (data not shown), indicating that the peak is due to aromatic residues in the N-
209 terminal OB-fold domain. The peak at 230 nm decreased when Dec monomers in 5 M urea were
210 shifted to 63 °C, consistent with Dec unfolding. When the sample was re-equilibrated at 33 °C,
211 the protein refolded rapidly as evidenced by regaining the positive 230 nm peak.

212 The high stability of the OB-fold was also observed in ¹H-¹⁵N HSQC spectra ([Figure 6B](#)).
213 The freshly purified Dec_{closed} trimer had only a handful of resonances at 33 °C in the absence of

214 urea. In the presence of 5 M urea there is a marked increase in resonances and the spectrum
215 has a chemical shift dispersion typical of folded proteins. Thus, the addition of 5 M urea appears
216 to dissociate the OB-fold domains from the Dec_{closed} state, allowing them enough rotational
217 diffusion freedom to be observed by NMR as is the case with acidic pH. The structure of the OB-
218 fold domains in the presence of 5 M urea was unfolded when the temperature was raised from 33
219 °C to 63 °C. The crosspeaks in the ¹H-¹⁵N HSQC spectrum collapse into the random coil region
220 of the spectrum between 7.7 and 8.7 ppm and the intensities of many crosspeaks decrease due
221 to fast hydrogen exchange from the unfolded state at high temperature. Returning the
222 temperature back to 33 °C gave a ¹H-¹⁵N HSQC spectrum indistinguishable from that at 33 °C
223 before heating, showing that thermal unfolding of the OB-fold domains is fully reversible. The OB-
224 fold domains of Dec monomers or Dec₁₋₉₈ also demonstrated reversible thermal unfolding ([Figure](#)
225 [6B](#)).

226 Taken together, these observations indicate that Dec refolding into the trimers
227 heterologously expressed and purified from *E. coli* is not strictly reversible and that the freshly
228 purified protein is in a state distinct from the re-trimerized protein. We are calling the initial state
229 Dec_{closed}, as opposed to the final trimer state Dec_{open} obtained by reassociating acid-induced
230 monomers at neutral pH ([see Figure 1B](#)). The operational distinction between Dec_{closed} and
231 Dec_{open} is that the latter is a trimer with independently tumbling OB-fold domains as evinced by
232 NMR signals from the majority of the residues in the protein, whereas the former Dec_{closed} is a
233 state where the OB-fold domains are rotationally restricted giving only a few NMR signals from
234 the chain termini. That the NMR spectrum of the initial Dec_{closed} is never recovered after exposure
235 to acidic pH or high temperature indicates that this is likely a misfolded state that results from
236 overexpression of the protein in a heterologous *E. coli* system.

237

238 [2.3 Characterization of the Dec C-terminal tail.](#)

239 The structure of the Dec C-terminal tail trimers is not well-defined in the cryoEM model of
240 Dec bound to phage L capsids (Newcomer et al. 2019). The C-terminal spike was homology
241 modeled as a β -helix when we first reported the structure of capsid-bound Dec (Newcomer et al.
242 2019). We reanalyzed the Dec trimer structure using AlphaFold2 (Jumper et al. 2021). The
243 predicted AlphaFold2 model has some striking differences from the original homology model.
244 Rather than the C-terminus forming a parallel β -helix, the AlphaFold2 model predicts an anti-
245 parallel β -sheet with high confidence (Figure 1E). Being agnostic about different modeling
246 approaches, we set out to obtain experimental evidence to assess the secondary structure of the
247 C-terminal spike using circular dichroism difference spectra. In Figure 7A, the spectrum of WT
248 Dec trimers at pH 7.4 is compared to that of Dec monomers made by acidification (each without
249 the His₆-tag). Thus, the difference spectrum (trimers – monomers) should correspond to the folded
250 trimeric C-terminal tails. Figure 7B shows the analysis of the difference spectrum using the
251 BeSTSeL secondary structure determination suite (Micsonai et al. 2022; Micsonai et al. 2018;
252 Micsonai et al. 2015). The fit of the difference spectrum indicates that the C-terminal tails have a
253 high probability for anti-parallel β -sheet (Figure 7C). The fit of the difference spectrum (NDec -
254 NDec₁₋₉₈) also supports that the C-terminal tails have antiparallel β -sheets (data not shown). In
255 all, the CD data are more consistent with the AlphaFold2 model than with our previous Dec model
256 that had a parallel β -helix as the C-terminal spike. However, we note that a potential difference is
257 that the CD data were obtained on Dec trimers freshly purified from *E. coli* that could conceivably
258 have a different C-terminal spike structure than Dec trimers bound to capsids. Another interesting
259 difference is that in the AlphaFold2 model the OB-fold monomers form more extensive contacts
260 between the protomers involving loops L₂₃, L₄₅, and the C-terminal helix (Newcomer et al. 2019)
261 that would probably bring the protomers too close to interact with the quasi-threefold binding site
262 on the P22 capsid. Thus, the OB-fold protomer interactions in the AlphaFold2 model may be more
263 relevant to the misfolded Dec_{Closed} conformation that leads to rotational restriction of the OB-fold

264 domains than to the functional Dec_{Open} conformation where the OB-fold domains are rotationally
265 independent. Note that the AlphaFold2 pLDDT confidence scores (Tunyasuvunakool et al. 2021)
266 are low (orange to yellow) for the OB-fold domain segments in the Dec trimer oligomerization
267 interface (Figure 1E).

268

269 3. DISCUSSION

270 The asymmetry of the Dec trimer structure is necessary for it to bind to coat proteins in
271 the mature virion. The binding modality of Dec to capsids is unique. It preferentially binds with
272 high affinity ($K_d = 9$ nM) to coat protein subunits at the capsid quasi three-fold axes of symmetry,
273 but specifically to those between hexons that cross a two-fold axis (Figure 1A) (Newcomer et al.
274 2019; Tang et al. 2006; Schwarz et al. 2015; Parent et al. 2012). The quasi three-fold sites
275 between hexons and pentons are never occupied by Dec, and the true three-fold axes can be
276 occupied but only at a much higher Dec concentrations because of the lower binding avidity (K_d
277 = 1.5 μ M) at these sites (Parent et al. 2012; Schwarz et al. 2015). We suggested this unusual
278 binding modality relates to the differing curvature of the capsid at these sites, such that the
279 curvature of the quasi three-fold axes between hexons and pentons precludes high avidity Dec
280 binding. Here, we hypothesize the unusual folding and assembly of Dec may be a consequence
281 of its need to bind to an asymmetric phage capsid binding site.

282

283 3.1 Dec monomers are capable of binding phage capsids.

284 The native gels in Figure 3 show that Dec trimerization is very slow, on the order of 4 days.
285 This is an unreasonably long time for a refolding reaction, especially for a phage protein being
286 synthesized in an infected cell that will lyse in less than an hour post-infection (Bode 1979). Our
287 data also showed that the Dec OB-fold domain alone, using NDec_{C1-98}, is insufficient for stable
288 binding to phage capsids (Figure 2C), suggesting that the C-terminal tail is essential for fortifying
289 Dec in its capsid-bound state.

290 We tested if full-length monomeric Dec could bind to phage capsids. Dec monomers were
291 formed by incubation at pH 1 and then the pH was shifted to 6 for 15 min. Phage P22 was added
292 to the Dec monomer sample and incubated for an additional 30 min before being applied to the
293 CsCl step gradient. Based on our *in vitro* refolding experiments (Figure 3B), this total incubation
294 time (~ 45 min) is insufficient for trimerization in solution. However, the full-length Dec monomers
295 bound phage capsids (Figure 2C), suggesting that the C-termini must trimerize in the presence
296 of phage capsids, thereby inducing stable binding.

297

298 3.2 The folding of Dec trimers is templated.

299 The folding of the Dec protein presents several conundrums. First, the Dec OB-fold
300 domain that directly interacts with the phage capsid is extremely stable and folds quickly. Yet the
301 C-terminal trimeric β -sheet spike is essential for binding of Dec to the phage capsids, but its
302 assembly into trimers is extremely slow. The timescale *in vitro* for trimer formation is several days
303 even at the high protein (0.25 mM) concentrations used in NMR experiments, whereas the
304 timescale of a phage L infection is less than an hour. We propose that *in vivo*, Dec monomers
305 bind to matured phage capsids via the OB-fold domain, and if binding occurs at the proper quasi-
306 three-fold symmetry sites between hexons, this templates the β -sheet trimer spike to lock the
307 complex and afford it additional stability. This may also be part of the reason that Dec does not
308 bind to immature procapsids where the particle curvature is different (Gilcrease et al. 2005). Thus,
309 capsid-templated trimerization overcomes the slow kinetics of Dec subunit association seen in
310 the absence of phages. It may be unfavorable for Dec subunit to associate in the absence of
311 phage since this might lock the trimer in a conformation that is sub-optimal to bind to the unusual
312 quasi-three-fold site on the capsid.

313 A second conundrum is the conformational state of trimeric Dec protein. The Dec_{closed}
314 conformation, which is the state of the protein when purified from cells overexpressing the protein,

315 is not the most thermodynamically stable form of the protein. We suggest that the Dec_{closed}
316 conformation could be a result of the high cytoplasmic Dec concentration and the absence of
317 phage particles. The very slow trimerization of Dec in the absence of phage capsids at the high
318 protein concentrations during overexpression may result in misfolding to the Dec_{closed} state. That
319 the Dec_{closed} state can be disrupted at acidic pH suggests that the misfolded state is stabilized by
320 electrostatic interactions. The interactions of Dec with P22 capsids are thought to be largely driven
321 by electrostatic interactions (Newcomer et al. 2019; Schwarz et al. 2015), so in the absence of
322 capsid improper electrostatic interactions may be the driving force favoring the misfolded Dec_{closed}
323 state. Indeed, the AlphaFold2 model (Figure 1E) predicts inter-protomer contacts that are not
324 present in the Dec trimer structure bound to phage capsids (Newcomer et al. 2019). However,
325 freshly purified Dec protein can bind to phage P22 mature virions, perhaps because interacting
326 with capsids shifts the protein to the Dec_{open} conformation, although we have not yet tested this
327 hypothesis experimentally. We suggest that the rotational freedom of OB-fold domains in the
328 Dec_{open} trimer is functionally required to bind to quasi three-fold symmetry sites on the capsid.

329 Templated folding is sometimes seen in intrinsically disordered proteins (IDPs), where
330 IDPs can be conformationally dynamic until a binding partner interacts, triggering a conformational
331 change allowing the structure to become ordered (Toto et al. 2020). Perhaps for phage L,
332 templated assembly overcomes the kinetic barrier for assembly of the C-terminal spike and allows
333 for binding specificity. In terms of nanotechnology, this unique templating feature may be useful
334 for making mixed chimeras with different proteins or probes attached to the C-termini that would
335 only interact once bound to a capsid.

336

337 **4. MATERIALS AND METHODS**

338 **Cloning and protein purification**

339 Full-length N-His₆ Dec isotopically enriched with ¹⁵N was expressed and purified as
340 previously described (Newcomer et al. 2018). To generate Dec monomers, freshly purified

341 NDec_{closed} trimers (pH 7.4, 14.1 mg/mL) were subjected to acidification to pH 1-2 for 30 minutes
342 at 22 °C, and subsequent titration back to pH 6. The NDec₁₋₉₈ mutant was prepared using purified
343 N-His₆ Dec plasmid DNA from a DH5α bacterial culture that was obtained using a StrataPrep
344 plasmid miniprep kit (Agilent Technologies). Replacing codon 99 with a stop codon was
345 accomplished by site-directed mutagenesis, using the primer pair 5'-
346 GTTCAGTAGCTAATGCAGAGAC and 5'-CGGGCAGTAGATAACTTATCCTAC (D'Lima and
347 Teschke 2015; Gilcrease et al. 2005). The construct was verified through DNA sequencing by
348 Genewiz (South Plainfield, New Jersey) and then transformed into *Escherichia coli* BL21(DE3)
349 cells for expression.

350 The expression and purification of NDec₁₋₉₈ was similar to the purification of NDec with a
351 few exceptions (Newcomer et al. 2018). After sedimentation, cells were resuspended in 20 mM
352 sodium phosphate, pH 7.6, containing a 1:100 dilution of protease inhibitor cocktail (Sigma),
353 0.15% w/v Triton, 7 mM MgSO₄, and 0.7 mM CaCl₂ (lysozyme, DNase and RNase were omitted).
354 Cells were lysed using a Constant One Shot Cell Disrupter, set to 30 psi. The purified Dec was
355 concentrated by gentle shaking over poly(ethylene glycol) (Aldrich, average MW 20,000)
356 in Spectra/Por dialysis tubing (8 kDa).

357

358 **NMR experiments**

359 NMR data were collected on a 600 MHz Varian Inova spectrometer (Palo Alto, CA)
360 equipped with a cryogenic probe, except for NMR experiments studying the combined effects of
361 temperature and urea which were performed on a 500 MHz Bruker Avance (Billerica, MA)
362 spectrometer. Unless otherwise noted, all samples were analyzed at a temperature of 33°C in
363 aqueous (90% H₂O/10% D₂O) 20 mM sodium phosphate buffer, pH 6, 50 mM sodium chloride.

364 NMR experiments monitoring irreversible dissociation of Dec at acidic pH (Figure 4) were
365 done on a 0.2 mM Dec trimer sample. NMR experiments following the reassociation of Dec from
366 monomers to trimers with time (Figure 5) were done with a 0.25 mM sample. The sample was

367 acidified to pH 1.9 for 30 min followed by raising the pH to 6.0 and collecting HSQC spectra at
368 various time points, NMR experiments investigating the thermal unfolding of Dec (Figure 6B) were
369 done on 0.2 mM, 0.6 mM and 1 mM samples of Dec_{closed}, Dec monomers and Dec_{C1-98},
370 respectively. For this experiment, after collecting an initial spectrum at 33°C, urea was added to
371 sufficiently destabilize the protein so that thermal unfolding could be observed. The 5 M urea
372 concentration was determined using a refractometer (Carl Zeiss, Germany) according to the
373 equation

$$374 \quad [urea] = \frac{\zeta - 1.3332}{0.00837}$$

375 where ζ is the refractive index (Pace 1986). After addition of 5 M urea the temperature was raised
376 to achieve unfolding and lowered to check reversibility.

377 NMR spectra were processed and analyzed using iNMR (<http://www.inmr.net>) and
378 CCPNmr Analysis (Vranken et al. 2005). Chemical shifts of NDec₁₋₉₈ were identified through
379 comparison with previously published assignments of the Dec monomer (Newcomer et al. 2018).

380

381 **Purification of WT bacteriophage P22**

382 To purify WT bacteriophage P22, *Salmonella enterica* serovar Typhimurium DB7136
383 (sup⁰, leu414(am), hisC527(am)) overnight cultures were diluted 1:100 in LB Super Broth [3.2%
384 tryptone, 0.5% yeast extract, 0.5% NaCl, 7 mM NaOH] and grown to an O.D. of 0.2 at 30 °C
385 (Botstein and Matz 1970). The cells were infected with WT P22 c1-7 (Levine 1957) (the c1-7
386 mutation prevents lysogeny) at a multiplicity of infection (MOI) of 0.1. The infected cultures were
387 grown at 30°C for an additional 6 hours or until lysis occurred. The cultures were chilled on ice
388 and chloroform was added to ensure complete cell lysis. The cell debris was pelleted by
389 centrifugation using a Sorvall F14-6 x 250 rotor for 10 minutes at 5,000 rpm. The supernatant was
390 transferred to an autoclaved flask containing 7% polyethylene glycol 8000 (Fisher) and 0.5 M
391 NaCl, and gently stirred at 4 °C overnight to precipitate the phage. The phage suspension was

392 pelleted by centrifugation at 8,000 rpm for 20 minutes at 4° C using the same rotor as above. The
393 phage-containing pellets were resuspended overnight in dilution fluid [20 mM Tris-HCl (pH 7.6),
394 100 mM MgCl₂] by gentle shaking at 4°C. The resuspended pellet was centrifuged at 10,000 rpm
395 for 10 minutes at 4 °C using a Sorvall F18-12 x 50 rotor to remove cell debris. The resulting
396 supernatant was ultracentrifuged at 45,000 rpm for 40 minutes at 4°C, and the phage pellet was
397 resuspended overnight in dilution fluid by gentle shaking. Any remaining cell debris was removed
398 via centrifugation at 10,000 rpm for 10 minutes at 4°C. The supernatant was transferred to a
399 sterile Falcon tube and stored at 4°C.

400 To further purify the phage sample and to separate mature virions from procapsids, the
401 clarified supernatant was applied to a CsCl (Sigma) step gradient (1.6 g/cc and 1.4 g/cc) with a
402 25% sucrose cushion (all solutions were prepared in dilution fluid). The gradients were spun in a
403 Sorvall MX120 ultracentrifuge (Thermo Fisher) at 18 °C for 60 minutes at 30,000 rpm. The phage
404 band was extracted from the gradient using a syringe and dialyzed against dilution fluid at 4°C
405 overnight using a Pur-A-Lyzer Mini 6000 (Sigma) dialysis tube. The phage stock was stored at
406 4°C.

407

408 **Dec binding to WT phage P22**

409 Aliquots of purified NDec₁₋₉₈ (pH 7.4, 1.16 mM), NDec trimers (pH 7.4, 0.98 mM) and Dec trimers
410 (pH 4; no His₆-tag, 0.12 mM protomers) were thawed on ice and spun in a Sorvall MX120
411 ultracentrifuge at 23,000 rpm for 15 minutes at 4°C to remove any aggregates. Dec monomers
412 were prepared by incubating the Dec trimers (pH 4) sample at pH 1 for 30 minutes at 22 °C. The
413 sample was then returned to pH 6 and allowed to incubate at 22 °C for 15 minutes (final
414 concentration, 0.097 mM). Following this incubation period, WT P22 (final concentration of 5 x
415 10¹² phage/mL) was simultaneously added to all protein samples. After mixing with the phage,
416 the final concentration of NDec trimers was 0.069 mM protomer and NDec₁₋₉₈ was 0.078 mM,
417 while the Dec monomer sample had a final concentration of 0.014 mM to decrease the possibility

418 of trimerization. The samples were nutated at 22 °C for 30 minutes then applied to CsCl step
419 gradients, as detailed above. The phage bands were puncture harvested using a syringe and
420 dialyzed overnight, as above. The proteins were TCA precipitated, resuspended in 3X SDS
421 sample buffer and analyzed on a 15% SDS polyacrylamide gel to determine if Dec bound to the
422 WT P22 virions.

423

424 **Time course of Dec trimerization and Dec stability**

425 An aliquot of Dec trimers (pH 4 , 0.12 mM initial concentration of protomers), in which the N-
426 terminal His₆-tag has been cleaved, was thawed on ice. Acid-induced unfolding of the Dec trimers
427 was achieved by adding small μ L aliquots of 1N HCl followed by vortexing until the pH decreased
428 to 1. The pH 1 sample was incubated at 22 °C for 30 minutes, followed by returning to neutral
429 pH by slowly titrating in 1N NaOH until the pH reached 6, where the final protein concentration
430 was 0.093 mM. The pH 6 sample was incubated at 33 °C and small aliquots were taken at
431 specified time points for analysis by native PAGE. The native PAGE gels were prepared in-house
432 using a 4.3% stacking gel and 15% separating gel. The native PAGE gels were run at 300V and
433 10 mA for 3 hours at 4°C to allow for sufficient separation of Dec trimers from Dec monomers.

434 To assess the long-term stability of Dec trimers, WT Dec (pH 6, 0.21 mM) without an N-
435 terminal His₆-tag was incubated at 33°C for 96 hours. A small aliquot was removed at specified
436 time points and assessed by native PAGE to determine the extent of protein denaturation that
437 occurs with time.

438

439 **Circular Dichroism of Dec**

440 Purified Dec trimers (pH 4) and Dec monomers, prepared as above, were diluted in
441 distilled water to a final protomer concentration of 0.2 mg/ml (0.013 mM). CD spectra were
442 acquired using a 0.1 cm path length quartz cuvette (Starna Cells, Inc.) on a Chirascan V100
443 spectrometer (Applied Photophysics). The CD spectra were collected from 190 to 260 nm at 22

444 °C with a bandwidth of 3 nm, 1 nm intervals and a time-per-point averaging of 5 seconds. The
445 oligomeric state of the WT Dec and WT Dec monomers was verified by native PAGE to ensure
446 that the CD spectra correspond to trimers and monomers, respectively.

447

448 **ACKNOWLEDGMENTS**

449 We thank Helen Belato for her help with the NMR Dec reassembly experiments. This work was
450 supported by NIH grant R01 GM07661 to CMT and by a grant from the UConn Research
451 Foundation to ATA and CMT.

452

453 **AUTHOR CONTRIBUTIONS**

454 A.T.A and C.M.T conceived of the project, directed the work, analyzed data and wrote the
455 manuscript. B.M.W. and R.L.N. did the experiments, analyzed the data, and contributed to the
456 writing of the manuscript.

457

458 **CONFLICT OF INTEREST**

459 The authors declare no potential conflict of interest.

460

461 **ORCID**

462 Andrei T. Alexandrescu <https://orcid.org/0000-0002-8425-9276>

463 Carolyn M. Teschke <https://orcid.org/0000-0001-6420-4895>

464

465

466 REFERENCES

- 467 Andersson, D., U. Carlsson, and P. O. Freskgard. 2001. 'Contribution of tryptophan residues to
468 the CD spectrum of the extracellular domain of human tissue factor: application in folding
469 studies and prediction of secondary structure', *Eur J Biochem*, 268: 1118-28.
- 470 Anfinsen, C. B. 1973. 'Principles that govern the folding of protein chains', *Science*, 181: 223-30.
- 471 Baker, D., and D. A. Agard. 1994. 'Kinetics versus thermodynamics in protein folding',
472 *Biochemistry*, 33: 7505-9.
- 473 Bode, W. 1979. 'Regulation of late functions in Salmonella bacteriophages P22 and L studied by
474 assaying endolysin synthesis', *J Virol*, 32: 1-7.
- 475 Botstein, D., and M. J. Matz. 1970. 'A recombination function essential to the growth of
476 bacteriophage P22', *J Mol Biol*, 54: 417-40.
- 477 Bryan, P. N., and J. Orban. 2010. 'Proteins that switch folds', *Curr Opin Struct Biol*, 20: 482-8.
- 478 D'Lima, N. G., and C. M. Teschke. 2015. 'A Molecular Staple: D-Loops in the I Domain of
479 Bacteriophage P22 Coat Protein Make Important Intercapsomer Contacts Required for
480 Procapsid Assembly', *J Virol*, 89: 10569-79.
- 481 Dedeo, C. L., C. M. Teschke, and A. T. Alexandrescu. 2020. 'Keeping It Together: Structures,
482 Functions, and Applications of Viral Decoration Proteins', *Viruses*, 12.
- 483 Ghosh, D. K., and A. Ranjan. 2020. 'The metastable states of proteins', *Protein Sci*, 29: 1559-
484 68.
- 485 Gilcrease, E. B., D. A. Winn-Stapley, F. C. Hewitt, L. Joss, and S. R. Casjens. 2005. 'Nucleotide
486 sequence of the head assembly gene cluster of bacteriophage L and decoration protein
487 characterization', *J Bacteriol*, 187: 2050-7.
- 488 Goodall, C. P., B. Schwarz, E. Selivanovitch, J. Avera, J. Wang, H. Miettinen, and T. Douglas.
489 2021. 'Controlled Modular Multivalent Presentation of the CD40 Ligand on P22 Virus-like
490 Particles Leads to Tunable Amplification of CD40 Signaling', *ACS Appl Bio Mater*, 4:
491 8205-14.
- 492 Haas, W., R. MacColl, and J. A. Banas. 1998. 'Circular dichroism analysis of the glucan binding
493 domain of Streptococcus mutans glucan binding protein-A', *Biochim Biophys Acta*, 1384:
494 112-20.
- 495 Jumper, J., R. Evans, A. Pritzel, T. Green, M. Figurnov, O. Ronneberger, K. Tunyasuvunakool,
496 R. Bates, A. Zidek, A. Potapenko, A. Bridgland, C. Meyer, S. A. A. Kohli, A. J. Ballard, A.
497 Cowie, B. Romera-Paredes, S. Nikolov, R. Jain, J. Adler, T. Back, S. Petersen, D.
498 Reiman, E. Clancy, M. Zielinski, M. Steinegger, M. Pacholska, T. Berghammer, S.
499 Bodenstein, D. Silver, O. Vinyals, A. W. Senior, K. Kavukcuoglu, P. Kohli, and D.
500 Hassabis. 2021. 'Highly accurate protein structure prediction with AlphaFold', *Nature*,
501 596: 583-89.
- 502 Kaplan, A. R., R. Olson, and A. T. Alexandrescu. 2021. 'Protein yoga: Conformational versatility
503 of the Hemolysin II C-terminal domain detailed by NMR structures for multiple states',
504 *Protein Sci*, 30: 990-1005.
- 505 Levine, M. 1957. 'Mutations in the temperate phage P22 and lysogeny in Salmonella', *Virology*,
506 3: 22-41.
- 507 Micsonai, A., E. Moussong, F. Wien, E. Boros, H. Vadaszi, N. Murvai, Y. H. Lee, T. Molnar, M.
508 Refregiers, Y. Goto, A. Tantos, and J. Kardos. 2022. 'BeStSel: webserver for secondary
509 structure and fold prediction for protein CD spectroscopy', *Nucleic Acids Res*, 50: W90-
510 W98.
- 511 Micsonai, A., F. Wien, E. Bulyaki, J. Kun, E. Moussong, Y. H. Lee, Y. Goto, M. Refregiers, and
512 J. Kardos. 2018. 'BeStSel: a web server for accurate protein secondary structure
513 prediction and fold recognition from the circular dichroism spectra', *Nucleic Acids Res*,
514 46: W315-W22.

- 515 Micsonai, A., F. Wien, L. Kernya, Y. H. Lee, Y. Goto, M. Refregiers, and J. Kardos. 2015.
516 'Accurate secondary structure prediction and fold recognition for circular dichroism
517 spectroscopy', *Proc Natl Acad Sci U S A*, 112: E3095-103.
- 518 Newcomer, R. L., H.B. Belato, C. M. Teschke, and A. T. Alexandrescu. 2018. 'NMR
519 assignments of the phage-cementing protein Decorator', *Biomol NMR Assign*, 12: 339-
520 43.
- 521 Newcomer, R. L., J. R. Schrad, E. B. Gilcrease, S. R. Casjens, M. Feig, C. M. Teschke, A. T.
522 Alexandrescu, and K. N. Parent. 2019. 'The phage L capsid decoration protein has a
523 novel OB-fold and an unusual capsid binding strategy', *Elife*, 8.
- 524 Pace, C. N. 1986. 'Determination and analysis of urea and guanidine hydrochloride denaturation
525 curves', *Methods Enzymol*, 131: 266-80.
- 526 Parent, K. N., C. T. Deedas, E. H. Egelman, S. R. Casjens, T. S. Baker, and C. M. Teschke.
527 2012. 'Stepwise molecular display utilizing icosahedral and helical complexes of phage
528 coat and decoration proteins in the development of robust nanoscale display vehicles',
529 *Biomaterials*, 33: 5628-37.
- 530 Porter, L. L., I. Artsimovitch, and C. A. Ramirez-Sarmiento. 2024. 'Metamorphic proteins and
531 how to find them', *Curr Opin Struct Biol*, 86: 102807.
- 532 Schwarz, B., P. Madden, J. Avera, B. Gordon, K. Larson, H. M. Miettinen, M. Uchida, B.
533 LaFrance, G. Basu, A. Rynda-Apple, and T. Douglas. 2015. 'Symmetry Controlled,
534 Genetic Presentation of Bioactive Proteins on the P22 Virus-like Particle Using an
535 External Decoration Protein', *ACS Nano*, 9: 9134-47.
- 536 Tang, L., E. B. Gilcrease, S. R. Casjens, and J. E. Johnson. 2006. 'Highly discriminatory binding
537 of capsid-cementing proteins in bacteriophage L', *Structure*, 14: 837-45.
- 538 Toto, A., F. Malagrino, L. Visconti, F. Troilo, L. Pagano, M. Brunori, P. Jemth, and S. Gianni.
539 2020. 'Templated folding of intrinsically disordered proteins', *J Biol Chem*, 295: 6586-93.
- 540 Tunyasuvunakool, K., J. Adler, Z. Wu, T. Green, M. Zielinski, A. Zidek, A. Bridgland, A. Cowie,
541 C. Meyer, A. Laydon, S. Velankar, G. J. Kleywegt, A. Bateman, R. Evans, A. Pritzel, M.
542 Figurnov, O. Ronneberger, R. Bates, S. A. A. Kohl, A. Potapenko, A. J. Ballard, B.
543 Romera-Paredes, S. Nikolov, R. Jain, E. Clancy, D. Reiman, S. Petersen, A. W. Senior,
544 K. Kavukcuoglu, E. Birney, P. Kohli, J. Jumper, and D. Hassabis. 2021. 'Highly accurate
545 protein structure prediction for the human proteome', *Nature*, 596: 590-96.
- 546 Uchida, M., B. LaFrance, C. C. Broomell, P. E. Prevelige, Jr., and T. Douglas. 2015. 'Higher
547 order assembly of virus-like particles (VLPs) mediated by multi-valent protein linkers',
548 *Small*, 11: 1562-70.
- 549 Vranken, W. F., W. Boucher, T. J. Stevens, R. H. Fogh, A. Pajon, M. Llinas, E. L. Ulrich, J. L.
550 Markley, J. Ionides, and E. D. Laue. 2005. 'The CCPN data model for NMR
551 spectroscopy: development of a software pipeline', *Proteins*, 59: 687-96.

552

553

554 **FIGURE LEGENDS**

555 **Figure 1. Dec structure and capsid binding sites. A)** Diagram showing the preferred quasi-
556 threefold binding-sites for Dec (yellow three-petal symbol) in the P22 T=7 icosahedral capsid. The
557 icosahedral 2-fold symmetry axes are designated by black bars. The arrangement of capsid
558 proteins into hexons and pentons is indicated by the green cages. A true 3-fold axis of symmetry
559 is denoted by the pink triangle. Dec prefers to bind to the quasi-3 fold axes of symmetry (yellow
560 three-petal symbol) across the 2-folds between hexons. It never binds to the quasi-3-fold
561 symmetry axes between hexons and pentons, indicated by the small cyan triangles. **B)** Schematic
562 illustrating the various states of the Dec protein described in this paper. In freshly purified Dec
563 trimers (Dec_{closed}), the OB-fold domains do not have rotational freedom. The OB-fold domains can
564 be released from the original Dec_{closed} conformation into the Dec_{open} conformation by incubation
565 at acidic pH. Further acidification unfolds the C-terminal spike and generates monomers that have
566 a folded OB-fold domain and an unfolded C-terminal tail. When the pH is reversed to pH 6,
567 trimerization is very slow ([Figure 3B](#)). **C)** Model of the NMR/cryoEM structure of the Dec trimer
568 with protomers colored purple, orange, and green (Newcomer et al. 2018; Newcomer et al. 2019).
569 In the left view, the globular OB-fold domains at the bottom of the structure contact the capsid.
570 The top of the structure is the spike that protrudes from the capsid surface and has lower
571 resolution in the cryoEM structure, indicative of higher flexibility. The spike was homology-
572 modeled as a three-stranded β -helix, but its structure has not been established experimentally
573 (Newcomer et al. 2018; Newcomer et al. 2019). An orthogonal 90°-rotated view is shown on the
574 right, with the β -helix spike colored gray. Note that the globular OB-fold domains have no contacts
575 with each other, and that the trimeric oligomerization state of capsid-bound Dec is maintained
576 primarily by interactions within the spike. **D)** The Dec_{1-98} deletion mutant has the C-terminal tail
577 genetically removed. The arrow indicates the position of residue 98. **E)** An AlphaFold2 (Jumper
578 et al. 2021) model of the trimeric Dec structure. The spike is predicted to have anti-parallel β -

579 barrel structure in contrast to the β -helix structure in the homology model (Figure 1C). In the
580 AlphaFold2 model each protomer contributes 3 anti-parallel strands to the spike, with parallel β -
581 sheet connections between the protomers. The interior of the β -barrel is not hollow but tightly
582 packed with hydrophobic residues.

583

584 **Figure 2. The C-terminal tail is required for capsid binding. A)** Non-denaturing polyacrylamide
585 gel (pH ~8.5) showing the oligomeric state of WT Dec trimers (T), Dec monomers (M), and NDec₁₋₉₈.
586 ₉₈ (Trunc). **B)** Superposition of NMR spectra for 1.7 mM NDec₁₋₉₈ (red) and 0.8 mM Dec monomers
587 (black). Both spectra were obtained at 33 °C for samples in 50 mM NaCl, 20 mM sodium
588 phosphate buffer, pH 6. The chemical shifts of residues in the OB-fold domains overlap indicating
589 the structure is conserved. The extra crosspeaks in the Dec monomers are from the unfolded C-
590 terminus (residues A99-S134), which is missing in NDec₁₋₉₈. **C)** SDS-PAGE analysis of Dec
591 proteins binding to phage P22 capsids. Purified NDec, NDec₁₋₉₈ or Dec monomers were incubated
592 with WT P22 phage for 30 min at room temperature then purified by CsCl step gradients. The
593 phage band was TCA precipitated and applied to a 15% SDS-PAGE gel to assess Dec binding.
594 Molecular weight markers (in kDa) are indicated on the left. The purified NDec, NDec₁₋₉₈ or Dec
595 monomers are depicted in the left panel. The right panel, denoted by the cyan box, shows NDec,
596 NDec₁₋₉₈ and WT Dec monomers that were incubated with WT P22 phages. The positions of NDec
597 and Dec monomers on the gel are denoted by purple and orange dots, respectively. The expected
598 position of NDec₁₋₉₈, which did not bind P22, is marked by a cyan dot with an X.

599

600 **Figure 3. Dec trimers are very stable yet take days to assemble. A)** WT Dec prepared in 20
601 mM sodium phosphate buffer pH 6 with 50 mM NaCl was thawed on ice and placed in a 33°C
602 incubator for 96 hours. Aliquots were removed at the times indicated and analyzed by native
603 PAGE, which showed that Dec maintains its trimeric state for up to 96 hours at pH 6 and a

604 temperature of 33 °C. **B)** By contrast, Dec monomers dissociated at acidic pH take days to
605 reassemble into trimers. Dec trimers (0.12 mM) were disassociated to monomers by incubation
606 at pH 1 for 30 min. The pH was readjusted to 6, and aliquots were taken at the times indicated for
607 analysis by native PAGE. For times up to 180 min, the aliquots were put on ice after incubation
608 at pH 6 and run on a single native polyacrylamide gel (shown on the left). For the longer time-
609 points, aliquots were taken from the incubation mixture every 24 hours for 4 days and run on
610 separate non-denaturing gels. A composite of the individual gel lanes is shown on the right.

611
612 **Figure 4. Disassembly of Dec_{closed} trimers into Dec monomers followed by NMR.** Starting
613 with a freshly purified 0.2 mM Dec trimer sample at pH 6 and 33 °C, the pH was lowered (down
614 arrows) and subsequently raised (up arrows) to the pHs indicated in each panel. At each pH a
615 ¹H-¹⁵N HSQC spectrum was recorded. The initial spectrum (top left) shows only a few crosspeaks
616 indicating the OB-fold domains are interacting in the trimeric Dec_{closed} state. As the pH is lowered,
617 NMR signals from the OB-fold domains appear, as the trimers disassemble into monomers (see
618 [Figure 2](#)). Adjusting the pH back to 6 does not result in the re-formation of Dec_{closed}.

619
620 **Figure 5. Reassembled Dec trimers have structurally independent OB-fold domains.** NMR
621 spectra of the trimeric Dec protein, dissociated at pH 2, show no changes in chemical shift
622 positions upon raising the pH back to 6 and incubating from 3 h (**A**) to 96 h (**B**). For comparison,
623 native PAGE show that most of the Dec monomer has reassembled to a trimer by 3-4 days,
624 indicating that the OB-fold domains in the reassembled trimeric Dec protein undergo free
625 rotational diffusion. We call this trimeric state Dec_{open} to distinguish it from Dec_{closed}, the freshly
626 purified trimer where NMR signals from the OB-fold segments are not observed indicating that
627 they interact in the trimer (Figure 4, pH 6 initial) **C)** A plot of the ratio of peak intensities at 3 h
628 compared to 96 h. Crosspeak intensities show a 2-fold decrease for residues in the C-terminal

629 tail compared to the OB-fold domain, suggesting the C-terminal domain signals are broadened
630 by conformational exchange or anisotropic tumbling of the spike component of the trimer.

631

632 **Figure 6. The globular OB-fold domains have a high stability to unfolding and reversible**

633 **folding. A)** Dec monomers were incubated in 0 or 5 M urea at 33 °C and circular dichroism

634 spectra were taken. Only the data from 220-260 nm are shown due to the absorbance of urea at

635 lower wavelengths. Addition of 5 M urea to Dec monomers does not affect the spectrum, indicating

636 that the OB-fold domain remains folded (compare black and pink lines and symbols). 5 M urea

637 was added for the thermal unfolding experiments because without denaturant the OB-fold

638 domains are so stable they need higher temperatures for unfolding, which results in protein

639 precipitation. Raising the temperature of the Dec sample in 5 M urea to 63 °C causes unfolding

640 of the OB-fold domain (cyan line). Shifting the sample back to 33 °C allows the protein to refold

641 the OB-fold domain, showing its unfolding is reversible (yellow and blue lines and symbols). **B)**

642 Unfolding and refolding of Dec_{closed} trimers, Dec monomers or Dec₁₋₉₈. On the left is the spectrum

643 of each protein in 0 M urea at 33 °C. Dec monomers and Dec₁₋₉₈ show the dispersed crosspeak

644 of the OB-fold domain, while in Dec_{closed} trimers the OB-fold domains interact resulting in few

645 crosspeaks. In the right three panels, the proteins are in 5 M urea, starting at 33 °C. Addition of 5

646 M urea to Dec_{closed} dissociates the OB-fold domains. Raising the temperature to 63 °C results in

647 the unfolding of the OB-fold domain. Returning the samples to 33 °C leads to rapid refolding of

648 the OB fold domain.

649

650 **Figure 7. The C-terminal spike of Dec trimers is consistent with the anti-parallel β -sheet**

651 **structure predicted by AlphaFold2. A)** Circular dichroism spectra of Dec trimers (blue), Dec

652 monomers (cyan) at 0.013 mM protomer concentration and 22 °C, and the difference spectrum

653 of trimers-monomers (orange) corresponding to the C-terminal spike of trimers. **B)** The fit (blue

654 line) of the difference spectrum (trimer-monomers, orange line) using BeStSel (Micsonai et al.

655 2022; Micsonai et al. 2018; Micsonai et al. 2015), with the residuals of the fit indicated by the gray
656 histogram. **C)** The distribution of structure types in the fit of the difference spectrum from BeStSel.
657
658

Figure 1

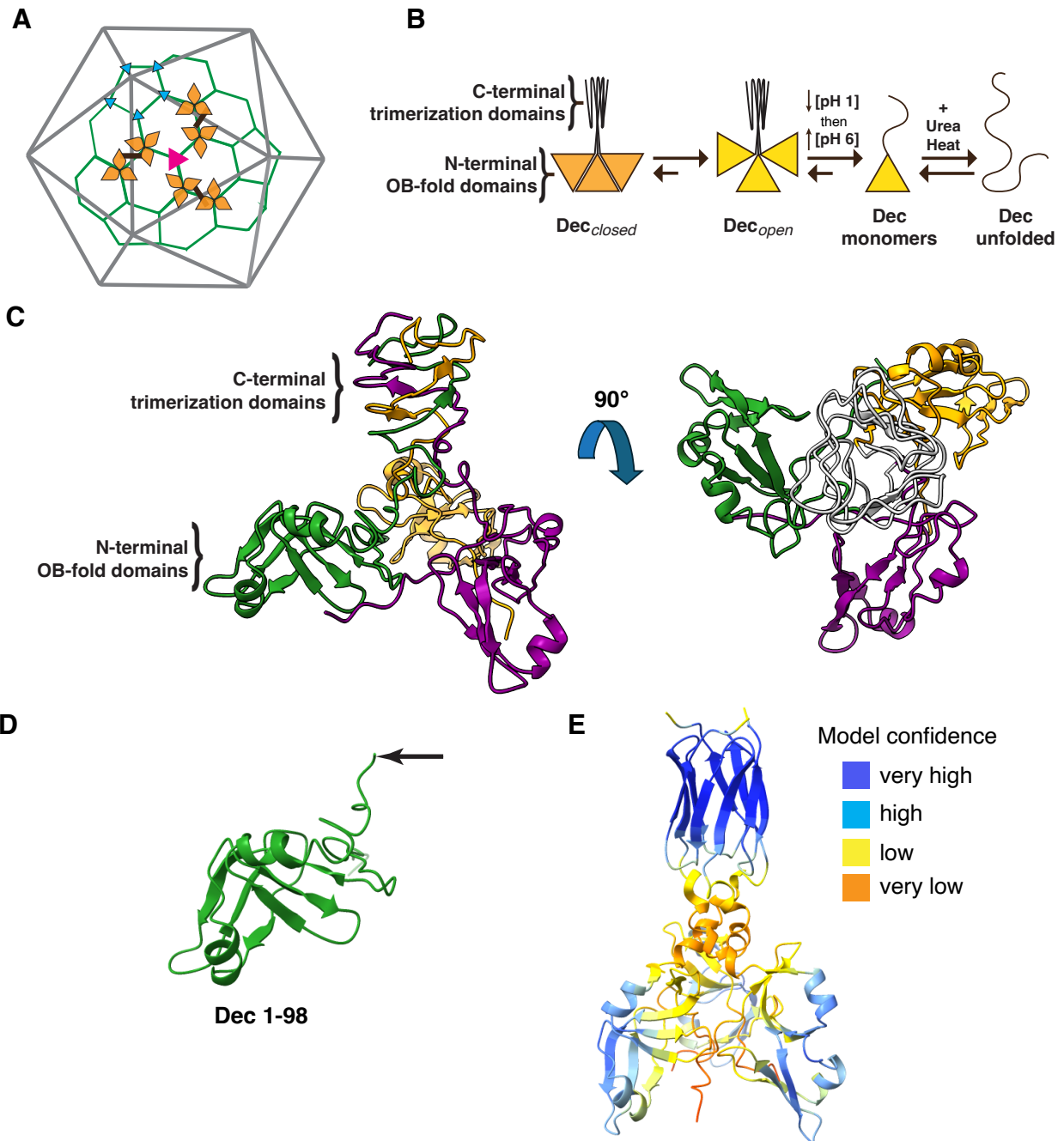


Figure 2

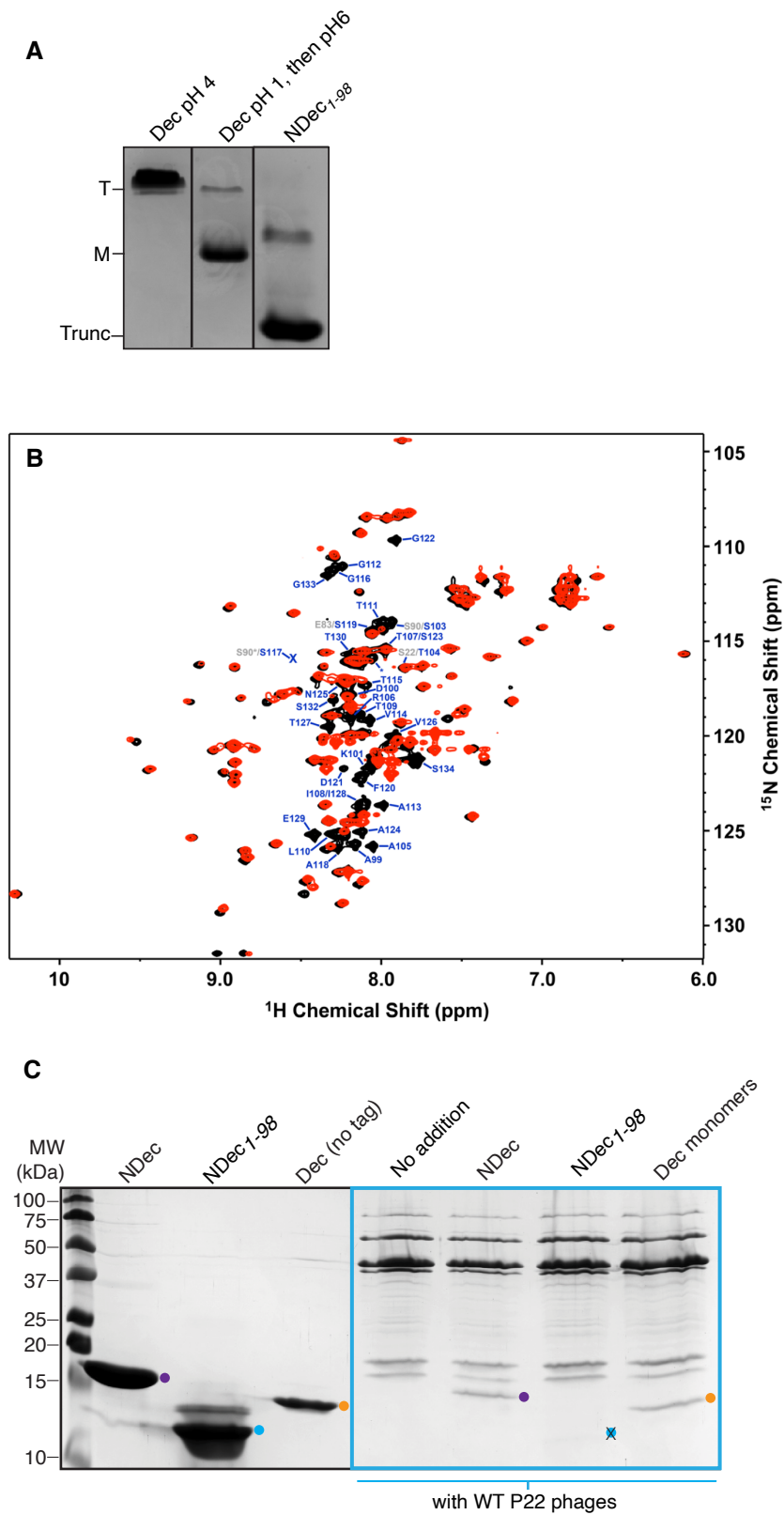


Figure 3

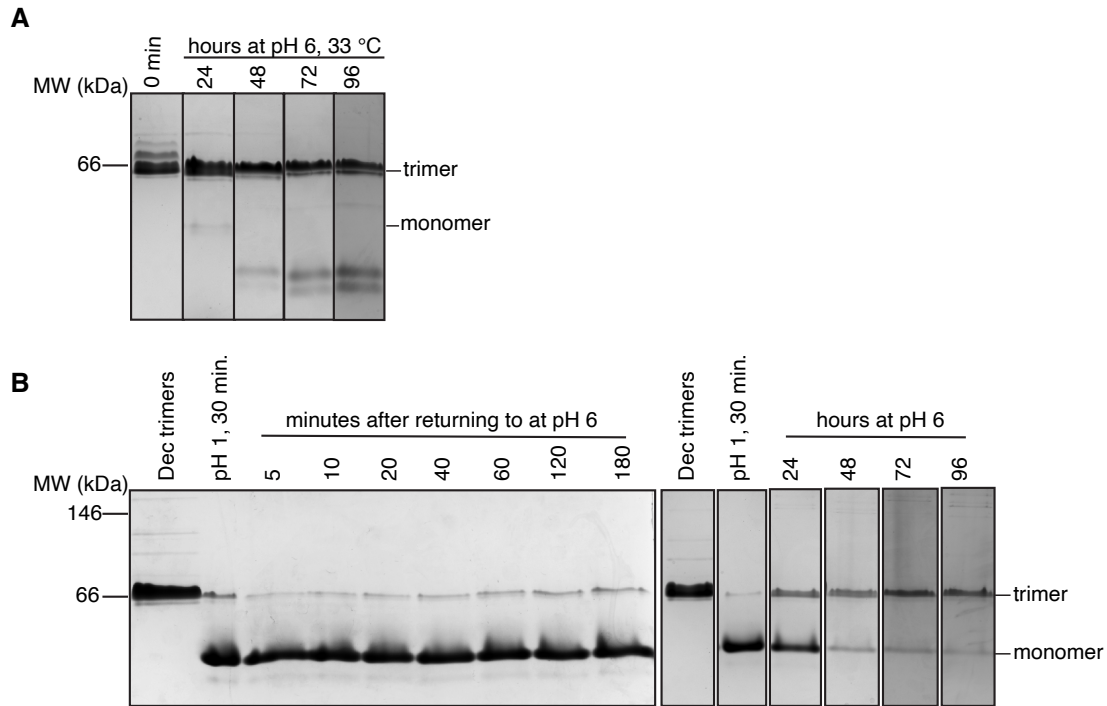


Figure 4

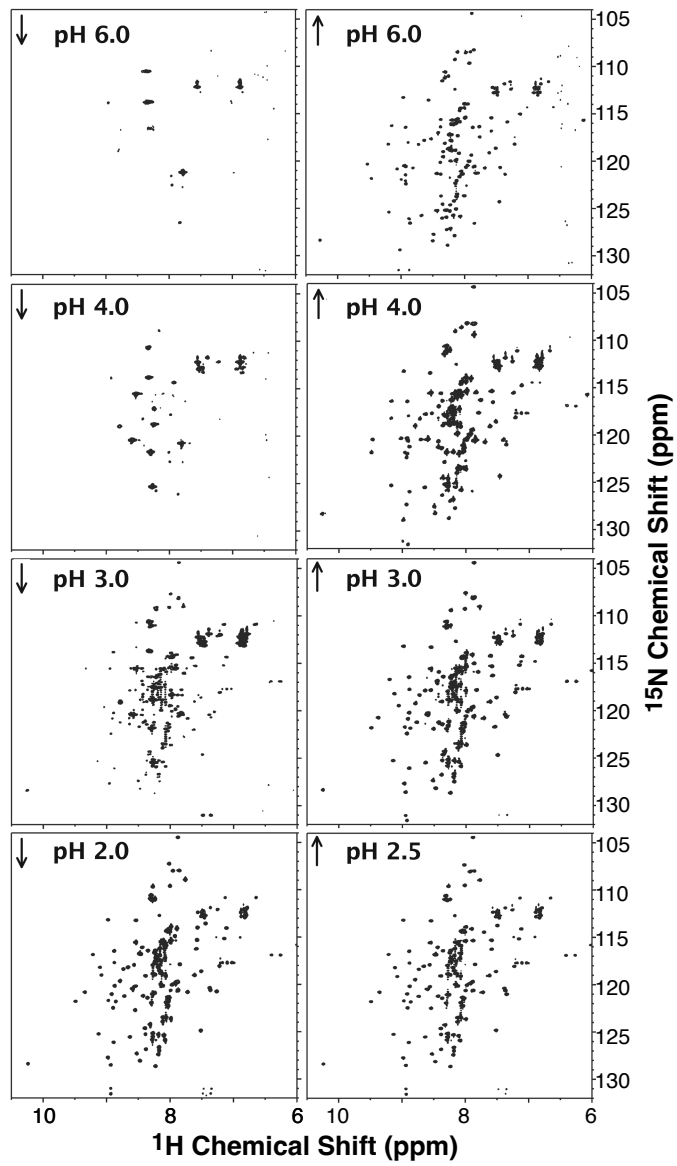


Figure 5

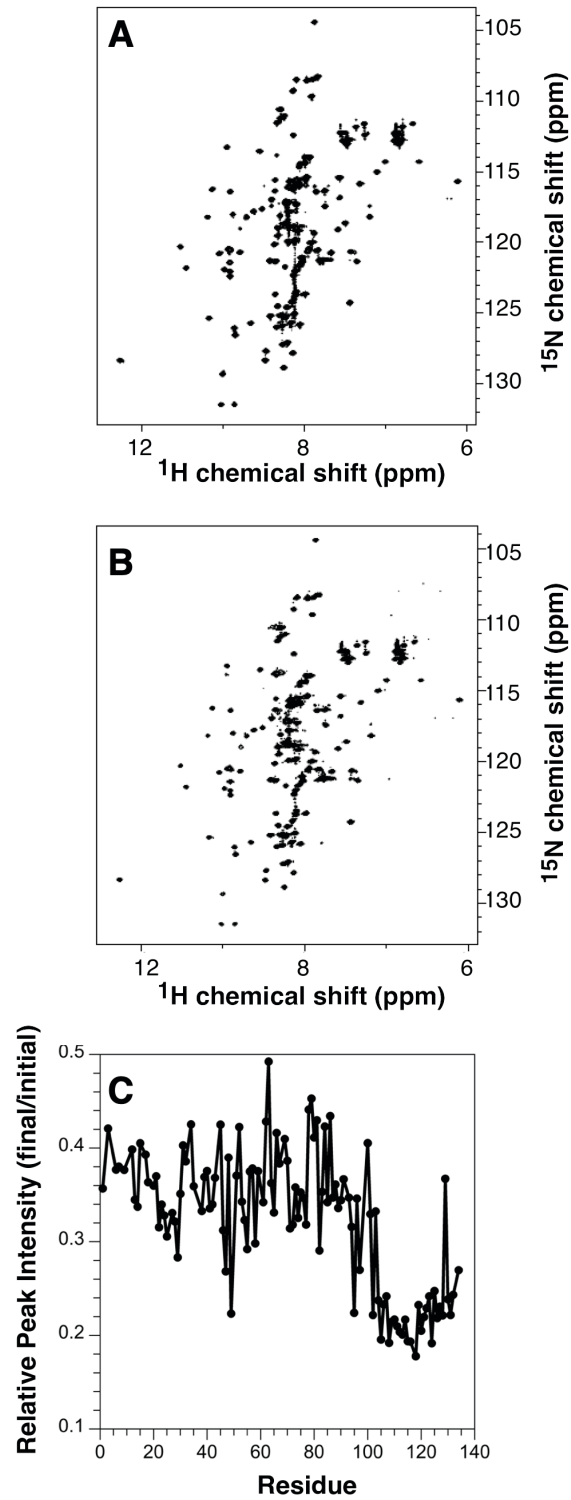


Figure 6

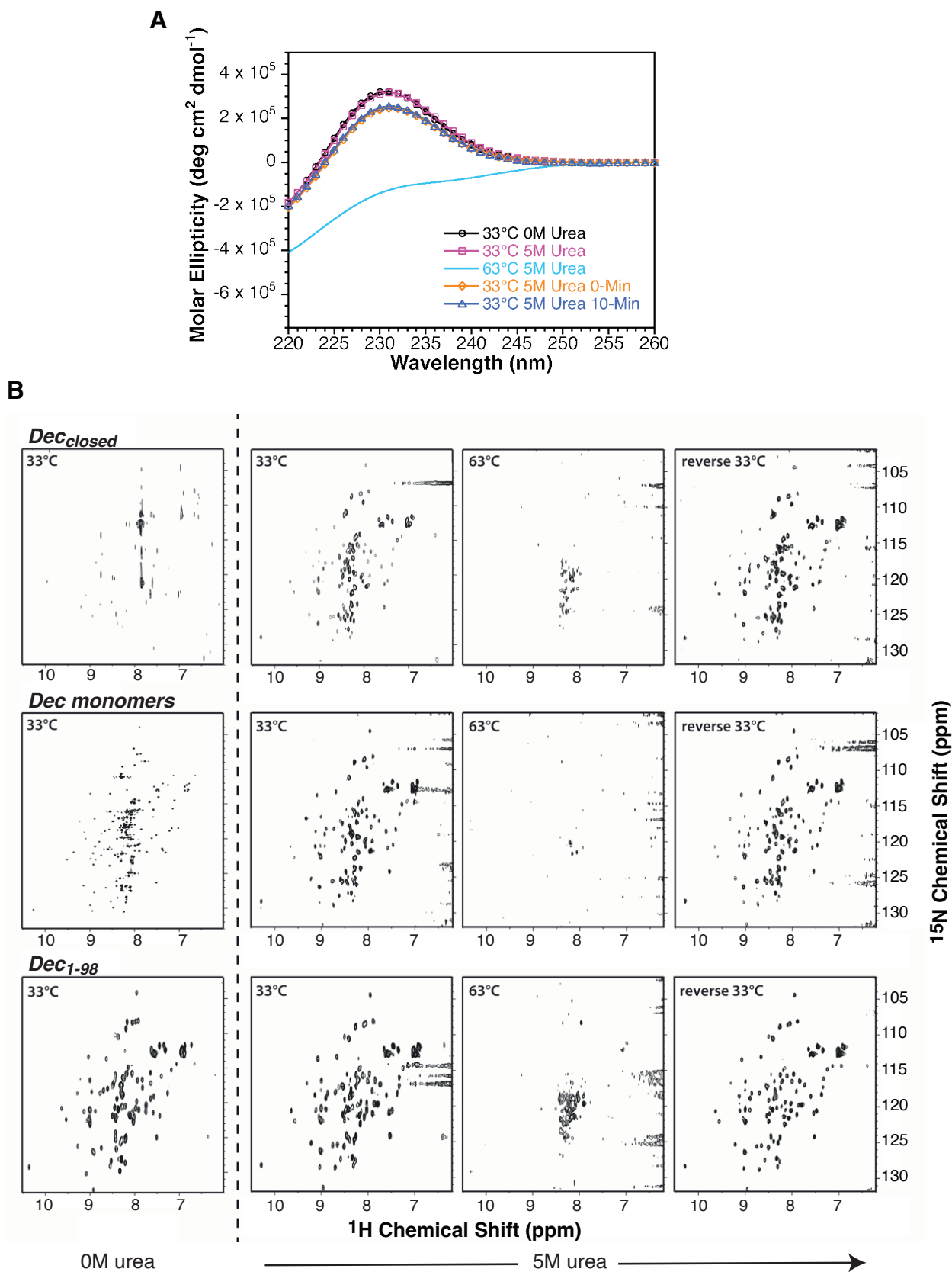


Figure 7

